MUTATION BIAS ALTERS THE DISTRIBUTION OF FITNESS EFFECTS OF MUTATIONS

Mrudula Sane[†], Shazia Parveen and Deepa Agashe*

Affiliation:

National Centre for Biological Sciences, GKVK Campus, Bellary Road, Bangalore 560065, India.

[†]Current affiliation:

Department of Ecology, Behavior and Evolution, University of California San Diego, San Diego, CA, USA

*Correspondence:

dagashe@ncbs.res.in

Short title: Mutation bias and fitness effects

ABSTRACT

Mutation bias is an important factor determining the diversity of genetic variants available for selection, and can therefore constrain the genetic paths to adaptation. An additional constraint emerges over the course of evolution. As adaptation proceeds and some beneficial mutations are fixed, new beneficial mutations become rare, limiting further adaptation. Recent theoretical work predicts that these constraints may be alleviated by a change in the direction of mutation bias (i.e., a bias reversal). As populations sample previously underexplored types of mutations, the distribution of fitness effects (DFE) of mutations should shift towards more beneficial mutations. Here, we test this prediction using *Escherichia coli*, which has a transition mutation bias, with ~55% of single-nucleotide mutations being transitions compared to the unbiased expectation of ~33% transitions. We generated mutant strains with a wide range of mutation biases from 96% transitions to 98% transversions, either reinforcing or reversing the wild type transition bias. Quantifying DFEs of hundreds of single mutations obtained from mutation accumulation experiments for each strain, we find strong support for the theoretical prediction. Strains that oppose the ancestral bias (i.e., with a strong transversion bias) have DFEs with the highest proportion of beneficial mutations, whereas strains that exacerbate the ancestral transition bias have up to 10-fold fewer beneficial mutations. Such dramatic differences in the DFE should drive large variation in the rate and outcome of adaptation. Our results thus strongly suggest an important and generalized evolutionary role for mutation bias shifts.

Keywords

Transition bias, DFE, mutational effects, DNA repair, mutation accumulation, mutation spectrum, GC bias.

INTRODUCTION

Mutation is the source of genetic variation in populations, and it is important to quantify the phenotypic and fitness effects of new mutations. A substantial body of work has therefore focused on determining the statistical distribution of mutational effects (the distribution of fitness effects, DFE) and the evolutionary processes that give rise to the DFE [1–3]. The DFE provides important information about the number and proportion of beneficial mutations, a key parameter in population genetic models of evolutionary change. A broad and general understanding of the DFE and factors that influence it is thus crucial to predict adaptation rates, trajectories, and fates of evolving populations. Ultimately, such predictions and their tests are key to tackling problems such as the emergence of antimicrobial resistance and rapid environmental change that threatens populations [4]. From numerous studies using different approaches to estimate or quantify the DFE [5], we know that it is influenced by several factors such as the genetic background, the environment, the effective population size, and prior history of adaptation [1–3,6,7].

New work in the past few years has suggested that the DFE may also vary with the nature of the underlying mutations. The mutation spectrum – describing relative frequencies of different types of mutations – is typically biased towards specific classes of mutations. For instance, most organisms show a bias towards more transition mutations [8]. If different mutational classes have distinct fitness consequences, such pervasive mutation biases may affect the DFE. For example, an *Escherichia coli* strain that samples a higher proportion of AT→CG transversion mutations had a distinct DFE for antibiotic resistance, compared to a strain that samples more GC→TA transversions [9]. During laboratory evolution under increasing antibiotic stress, strains with different mutational bias developed resistance using distinct mutational paths [10]. Expanding this idea to genome-wide mutational biases, we recently showed that changing the mutation bias can alter the *E. coli* DFE across several environments with limiting carbon sources [11]. Specifically, on deleting a DNA repair gene

(*mutY*) – which increases the incidence of transversion mutations compared to the wild type (WT) – we observed an ~6% increase in the fraction of beneficial mutations on average across environments. The form of the global DFE may thus change depending on the mutation spectrum of an organism and the fitness effects of different types of mutations.

Further, using adaptive walk simulations, we uncovered general conditions under which mutation bias shifts should change the DFE, and the evolutionary impacts of the expected DFE changes [11,12]. This led to a key prediction: opposing (i.e., reversing or reducing) the direction of the ancestral mutation bias should increase the fraction of beneficial mutations. Opposing the mutation bias is predicted to be generally beneficial because it allows populations to explore previously under-sampled mutational space, including beneficial mutations that were not fixed (and were therefore available). For instance, a population that has been evolving with a transition mutation bias (e.g., WT *E. coli*) will have already fixed many of the possible beneficial transition mutations, but would have sampled only a small fraction of beneficial transversions. On introducing a sudden transversion bias (reversing the existing bias), such a population could more easily sample beneficial transversions, leading to a right-shifted DFE. The more extreme the bias reversal, the higher the probability that the population will sample a beneficial transversion. In contrast, if the ancestral bias is reinforced (i.e., with a stronger transition bias in *E. coli*), we predict that the DFE should shift left compared to the WT, with a larger fraction of deleterious mutations. These predictions indicated important roles for mutation biases in shaping DFEs, and as a result, adaptive trajectories [11,12].

Here, we experimentally test these predictions by generating empirical DFEs of new mutations in six *E. coli* strains carrying deletions of various DNA repair genes, including the mismatch repair system (MMR) (Table 1). The lack of DNA repair leads to a wide range of mutation biases, with transversion biases of 0.04 (i.e., 96% transitions, Ts) to 0.98 (i.e., 98% transversions, Tv) [8,13]. To obtain single-step mutations, we allowed several lineages of

each strain to evolve independently in a mutation accumulation (MA) regime (partial results from MA experiments for WT and Δ*mutY* were described in [11,14]). Evolution under MA allows nearly all mutations to be sampled (but see [15,16]), allowing us to obtain a random representative sample of mutations available to each strain. We used whole-genome sequencing to identify lineages with a single mutation compared to the respective ancestor, measured the fitness effect of each mutation in two environments, and used these data to construct DFEs. Our results provide strong support for our predictions, demonstrating that mutation spectrum shifts can determine the amount of adaptive genetic variation available to populations.

METHODS

Bacterial strains

We obtained the wild-type (WT) strain of *E. coli* K-12 MG1655 from the Coli Genetic Stock Centre (CGSC, Yale University), streaked it on Luria Bertani (LB) agar (Miller), and chose one colony at random as the WT ancestor for subsequent experiments. We similarly obtained the mutator strains of *E. coli* (Δ*mutT*, Δ*mutH*, Δ*mutL*, Δ*mutS*, Δ*nth,* Δ*nei*, Δ*mutY*) from the Keio collection of gene knockouts from CGSC (BW25113 strain background [17]). These gene knockouts were made by replacing open reading frames with a Kanamycin resistance cassette, such that removing the cassette generates an in-frame deletion of the gene. The design of gene deletion primers ensured that downstream genes were not disrupted due to polar effects. For each mutator strain, we moved the knockout locus from the BW25113 background into the MG1655 (WT) background using P1 phage transduction [18]. We then removed the kanamycin resistance marker by transforming kanamycin-resistant transductants with pCP20, a plasmid carrying the flippase recombination gene and ampicillin resistance marker. We grew ampicillin resistant transformants at 42 ºC in LB broth overnight to cure pCP20 and streaked out 10 µL of these cultures on LB plates. After 24

hours, we replica-plated several colonies on both LB + kanamycin agar plates and LB + ampicillin agar plates, to screen for the loss of both kanamycin and ampicillin resistance. We PCR-sequenced the knockout locus to confirm removal of the kanamycin cassette. For generating the Δ*nth-nei* double knockout, we first created a Δ*nth* strain, and then moved the Δ*nei* locus into this background using P1-phage transduction as described above.

Mutation accumulation (MA) experiments

We used mutation accumulation (MA) experiments of varying length to obtain mutator strains carrying single mutations that would reflect the mutation spectrum of each mutator. We founded multiple MA lines of each strain from single colonies: WT (118 lines), Δ*mutT* (300 lines), Δ*mutH* (350 lines), Δ*mutL* (350 lines), Δ*mutS* (350 lines), Δ*mutY* (430 lines) *and* Δ*nth-nei* (300 lines) and propagated them through daily single-colony bottlenecks on LB agar plates (Table 1). We evolved WT lines in two sets: one set of 38 lines evolved for 300 days (8250 generations, described previously in [11,14]), and the second set of 80 lines evolved for 85 days (2295 generations) (Table S1). Next, we evolved the mutators with intermediate mutation rates in short MA experiments: Δ*nth-nei* in a single set (8 days, ~216 generations), and Δ*mutY* in three sets (set 1: 300 lines, 10 days, ~270 generations, described previously in [11]; set 2: 80 lines, 5 days, ~135 generations; set 3: 50 lines, 1 day, ~27 generations; Table S1). We evolved mutators with very high mutation rates (Δ*mutT*, Δ*mutS*, Δ*mutL*, Δ*mutH*) for a single day (~27 generations). The MA protocol minimises the effect of selection, allowing sampling of a wide range of mutational effects, largely independent of their fitness consequences. For each MA line, every 24 hours we streaked out a random colony (closest to a pre-marked spot) on a fresh LB agar plate. For MA experiments lasting more than a day, every 4-5 days we inoculated a part of the transferred colony into LB broth at 37ºC for 2-3 hours and froze 1mL of the growing culture with an equal amount of 60% glycerol at –80ºC. For 1-day MA experiments, we similarly cultured

and froze the final chosen colony. We used these freezer stocks of the MA lines for sequencing.

Whole-genome sequencing to identify single mutations and determine mutation spectra

We sequenced individual colonies from the MA experiments to identify all clones carrying only a single mutation relative to their ancestor. For WT, Δ*nth-nei* and Δ*mutY*, we inoculated 2µL of the frozen stock of each evolved MA line into 2mL LB, and allowed the cells to grow overnight at 37ºC with shaking at 200 rpm. For Δ*mutT*, Δ*mutH*, Δ*mutL* and Δ*mutS*, we allowed cells from frozen stocks to only grow for 3-4 hours in 2mL LB (37ºC, 200 rpm), to minimize the accumulation of additional mutations. Next, we extracted genomic DNA (GenElute Bacterial Genomic DNA kit, Sigma-Aldrich) and quantified it using the Qubit HS dsDNA assay kit (Invitrogen). We prepared paired-end libraries from each line and the MA ancestors, and sequenced them on an Illumina platform (either 2x100 bp, or 2x125 bp, or 2x250 bp). Table S1 provides details of the library preparation and sequencing methods used in this study. In some cases, whole genome sequencing (WGS) for some MA lines was unsuccessful, i.e., we obtained a very small number of reads; these lines were excluded from further analyses (Table 1). For each sample where WGS was successful, we aligned quality-filtered reads to the NCBI reference *E. coli* K-12 MG1655 genome (RefSeq accession ID GCA_000005845.2) and generated a list of base-pair substitutions and short indels (<10bp) using Breseq [19] and VarScan [20,21]. Finally, we removed ancestral mutations from the mutation lists of evolved lines.

We estimated mutation rate and mutation bias for each mutator and WT using mutations called from all sequenced isolates (Table 1, row “MA lines successfully sequenced”). We calculated mutation rates (per bp per generation) as the total number of mutations in a particular strain (Table 1, row “Total mutations in sequenced lines”) / (Genome size (4.6 x

10^6) * Total number of generations elapsed in the MA experiment). The total number of generations elapsed in the MA experiment is calculated as the number of days of evolution x number of generations per day x number of lineages for which mutation information was available (Table S1). We calculated mutational biases from the different types of mutations observed in the MA-evolved lines (Table 1) as described in [11]. For instance, we calculated the Tv bias as the number of transversions/(number of transitions + number of transversions). Similarly, we calculated the GC→AT bias as the number of GC→AT mutations/(number of AT→GC mutations + number of GC→AT mutations).

From the complete set of all MA-evolved lines with WGS, we filtered those that had a single new mutation compared to the respective ancestor. This included 92 clones of Δ*mutS*, 97 Δ*mutL*, 100 Δ*mutH*, 102 Δ*nth-nei*, 94 WT (80 from set 1 [14] and 14 from set 2), 113 Δ*mutY* (79 from set 1 [11], 26 from set 2 and 8 from set 3), and 97 Δ*mutT* MA lines (Table 1, row "MA lines with single mutations"). We performed all fitness assays and subsequent analyses (described below) with these 695 isolates.

Growth rate measurements to construct single-mutation DFEs

We measured growth rates of each evolved MA line with a single mutation and its respective ancestor in two liquid culture media: LB broth (Miller, Difco) or M9 minimal salts (Difco) + 5 mM glucose. We inoculated each isolate from its freezer stock into either LB broth or M9 minimal salts medium with 5mM glucose, and allowed it to grow at 37 ºC with shaking at 200 rpm for 14-16 hours. We inoculated 2 µL of this culture into 200 µL growth media in 96-well plates (Costar) and incubated the well plate in a Tecan F200 Multimode plate reader at 37ºC with orbital shaking at 185 rpm for 16-18 hours. Every 15 minutes, the plate reader measured the optical density (OD600) for all wells. In each plate, we included the MA ancestors relevant for the evolved MA isolates to enable fitness calculations, a reference strain (the parent WT strain) to enable checks for consistency across plate reader runs, and

blank control wells to check for media sterility. For each evolved isolate, we used the average growth rate of three technical replicates to calculate the relative growth rate as: growth rate of evolved strain/growth rate of ancestral strain. For WT MA lines, we used the WT ancestor; and for mutator MA lines, we used the mutator ancestor. We estimated maximum growth rate, obtained from a linear fit to log OD600 vs. time curves, using the Curve Fitter software [22]. The fitness effect of each mutation (*s*) was then calculated as relative growth rate – 1, which is equivalent to (growth rate(evolved) – growth rate(ancestor)) / growth rate(ancestor). We used *s* values of mutations to construct strain and environment-specific distributions of fitness effects (DFE). Finally, we corrected our DFEs for the expected selection bias in bacterial colonies in MA experiments as described before [11,15]. The bias-corrected vs. uncorrected DFEs are shown in Figures S1 and S2.

Table 1: Strains used in this study, and their mutational characteristics. For each class of mutations, bias is calculated as (no. of mutations of type A) / (no. of mutations of type A + no. of mutations of type B). Brief information about the function of deleted genes is provided in the footnotes [48].

Property	**ΔmutS**	**ΔmutL**	**ΔmutH**	**Δnth-nei**[Ψ]	**WT**	**ΔmutY**	**ΔmutT**
MA lines evolved	350	350	350	300	98	430	300
MA lines successfully sequenced	345	344	346	285	97	424	272
Total mutations in sequenced lines [a]	616	603	908	502	426	798	789
MA lines with single mutations [b]	92	97	100	102	94 [c]	113	97
Mutation rate ($\times 10^{-8}$)	1.4	1.4	2.1	0.17	0.0091	0.094	2.3
BPS	508	509	809	482	387	787	783
Indel	108	94	99	20	39	11	6
Indel bias	0.18	0.16	0.11	0.04	0.09	0.01	0.01
Coding	440	437	710	400	282	684	657
Noncoding	68	72	99	82	105	103	126
Noncoding bias	0.13	0.14	0.12	0.17	0.27	0.13	0.16
Non-synonymous	290	274	433	273	183	489	462
Synonymous	150	163	277	127	99	195	195
Synonymous bias	0.34	0.37	0.39	0.32	0.35	0.29	0.30
Transitions	491	491	774	430	206	69	12
Transversions	17	18	35	52	178	644	771
Transversion bias	0.03	0.04	0.04	0.11	0.46	0.91	0.98
AT→GC	339	361	568	22	118	24	775
GC→AT	162	143	229	438	206	746	5
No change	7	5	12	22	60	17	3
GC→AT bias	0.32	0.28	0.29	0.95	0.64	0.97	0.01

[a] Mutations used to calculate mutation rates and spectra.
[b] Lines used for fitness measurements and inference of DFEs.
[c] Of the 94 mutations, 46 are second-, third-, or fourth-step mutations occurring in a given lineage, whose fitness effect was estimated with respect to the immediate ancestor (i.e., carrying first- or second- step mutations, respectively). Details are described in [14].
[] Genes involved in the methyl-directed mismatch repair (MMR) pathway. MutS recognizes mismatched base-pairs in double stranded DNA. MutL binds to DNA-bound MutS, and facilitates interaction with MutH. MutH performs daughter-strand recognition and creates single-strand DNA breaks in the daughter strand at the nearest hemi-methylated site. The breaks are then repaired by exonuclease activity extending up to the mismatch, followed by resynthesis by DNA polymerase III.
[Ψ] Genes involved in the repair of damaged pyrimidines in double-stranded DNA. *nth* encodes Endonuclease III, which recognizes and cleaves N-glycosidic bonds of damaged pyrimidines, leaving abasic sites, and also cleaves the phosphodiester backbone 3' to the site to create single-strand DNA breaks. *nei* encodes Endonuclease XIII, and shares specificity with Endonuclease III.
[] Genes involved in the 8-oxo-dGTP repair pathway. MutT hydrolyses cytosolic 8-oxo-dGTP to 8-oxo-dGMP, preventing its incorporation into DNA during replication. MutY recognizes 8-oxo-G:A mis-pairs in double-stranded DNA and excises the adenine, leaving an abasic site.

RESULTS

Transversion-biased strains have a right-shifted distribution of fitness effects (DFE) with a higher proportion of beneficial mutations and lower deleterious load

To test our hypothesis that transversion-biased *E. coli* strains can access more beneficial mutations, we constructed single-mutation DFEs for strains with a range of transition/transversion biases (Table 1). For each strain, we characterized the fitness effects of a total of ~100 single mutations in two growth media: one rich (LB) and one relatively poor (minimal medium with glucose), using exponential growth rate as a measure of fitness. The median selection coefficient of single mutations varied from –0.16 to +0.038 (i.e., a 16% reduction to 3.8% increase in growth rate) in LB, and from –0.013 to +0.063 (i.e., 1.3% reduction to 6.3% increase in growth rate) in glucose. As predicted, in both environments, strains that reinforced the WT (ancestral) mutation bias (i.e., were strongly Ts-biased: Δ*mutS*, Δ*mutL*, Δ*mutH* and Δ*nth- nei*) had left-shifted DFEs relative to WT (Figures 1 and 2). In contrast, the DFEs of strains that opposed the WT mutation bias (i.e., had a strong Tv bias, Δ*mutY* and Δ*mutT*) had right-shifted DFEs. The DFE differences across strains were reflected in the proportion of beneficial mutations (f_b), which was significantly higher in Tv-biased vs. Ts-biased strains (Figure 3A; Table S2, Table S3), and increased with Tv bias (Figure S3A–B). Concomitantly, the fraction of deleterious mutations (f_d) was significantly lower in Tv-biased strains (Figure 3A; Table S2, Table S3) and tended to reduce with increasing Tv bias in both growth media, though the relationship was not statistically significant (Figure S3C–D). Despite these overall trends, we note some exceptions. In LB, Δ*nth-nei* had much higher f_b than strains with both higher and lower Ts bias (Table S2). In glucose, Δ*mutL* and Δ*mutH* had higher f_b values despite the same transition bias as Δ*mutS* and a stronger Ts bias than Δ*nth-nei* (Table S3). We explore these exceptions in more detail in the discussion section.

An important consequence of increased genomic mutation rates is that mutators enjoy an increased total beneficial mutation supply (S_b), but must also contend with higher deleterious genetic load (L_d) – both important factors in determining their fates during adaptation [23–25]. We first calculated S_b and L_d for all strains assuming WT f_b and f_d (i.e., assuming similar DFEs across strains) [26]. As expected, these values scale linearly with the genomic mutation rate, with strains with 100x higher mutation rates predicted to have a 10–250-fold greater beneficial supply and lower deleterious load compared to WT (Figure S4, Tables S4–S5). However, on accounting for the altered f_b and f_d values of mutator strains due to their DFE shifts, we observed deviations from this relationship. Ts biased strains typically had lower S_b while Tv biased strains had higher S_b than expected (Figure S4A and S4B, compare open circles vs. filled circles; Table S4). The pattern for L_d was opposite: Ts biased strains had a higher L_d, and Tv biased strains had a lower L_d than expected based on mutation rate alone (Figures S4C and S4D, Table S5). The effect of using the empirically observed DFEs was strongest for Δ*mutT*, where the beneficial supply relative to wild type increased from ~250 fold to ~700 fold and ~400 fold in LB and glucose respectively (Table S4), and the deleterious load reduced from ~250 fold to ~90 fold in LB and ~60 fold in glucose (Table S5). Thus, mutation bias shifts could have very large effects on the evolutionary fate of mutators.

Figure 1: Distribution of fitness effects of new mutations in a rich medium (Luria Bertani broth, LB) for *E. coli* strains with varying mutation bias. The distribution of fitness effects of single randomly occurring mutations in each strain (sample size in parentheses), calculated as maximum growth rate relative to the respective ancestor (x-axis). The schematic at bottom right shows the transversion (Tv) bias of each strain. The WT strain is shown in cyan; strains that reinforce the WT transition bias are in purple; strains that reduce or reverse the WT bias (i.e., have a transversion bias) are in pink. Each DFE was corrected for selection bias as described in [15]; raw (uncorrected) DFEs are shown in Figure S1; raw fitness values are provided in Supplemental data file S1. Grey areas indicate neutral mutations (s=0±0.025 to account for experimental measurement error); bold lines and numbers indicate median values of s.

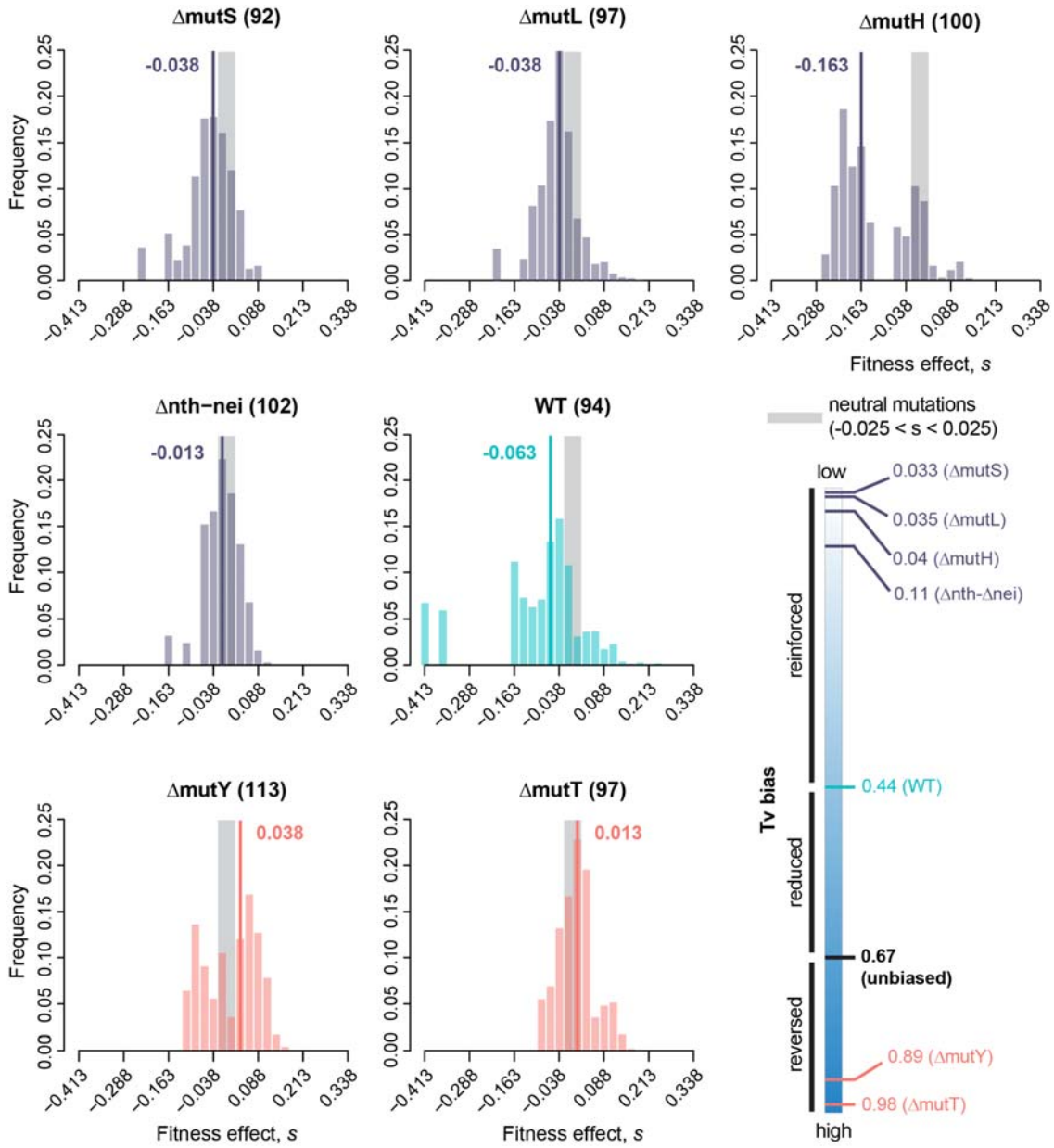

Figure 2: Distribution of fitness effects of new mutations in a minimal medium (M9 broth with 5 mM glucose) for *E. coli* strains with varying mutation bias. The distribution of fitness effects of single randomly occurring mutations in each strain (sample size in parentheses), calculated as maximum growth rate relative to the respective ancestor (x-axis). The schematic at bottom right shows the transversion (Tv) bias of each strain. The WT strain is shown in cyan; strains that reinforce the WT strain's transition bias are in purple; strains that reduce or reverse the WT bias (i.e., have a transversion bias) are in pink. Each DFE was corrected for selection bias during MA as described in [15]; raw (uncorrected) DFEs are shown in Figure S2; raw fitness values are provided in Supplemental data file S2. Grey areas indicate neutral mutations (s=0±0.025 to account for experimental measurement error); bold lines and numbers indicate median values of s.

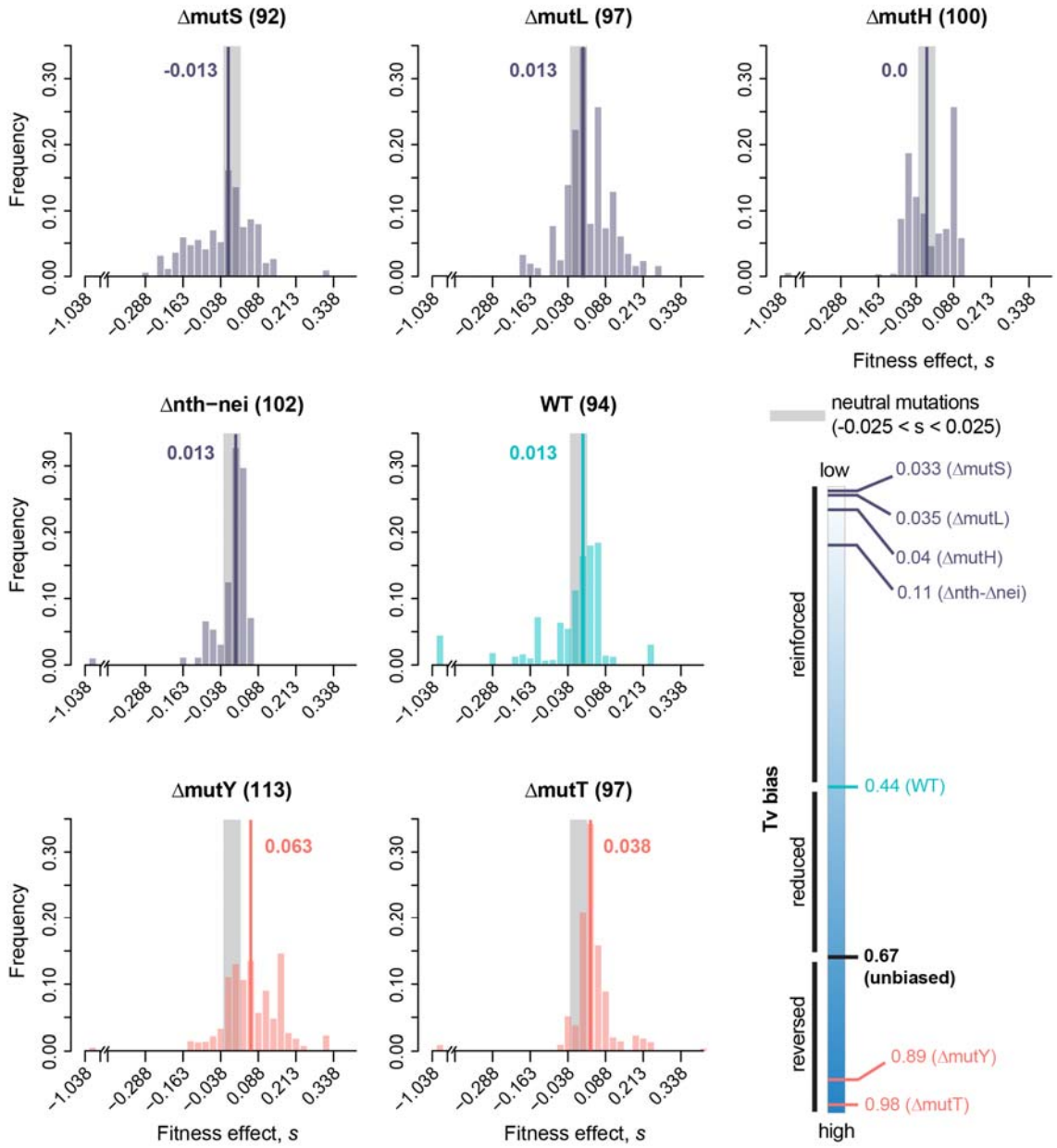

Figure 3: Differences in DFEs of strains are most strongly associated with transversion bias. (A) Stacked bar plots show the total fraction of neutral, deleterious, and beneficial mutations observed in the DFEs of each strain in each growth medium, extracted from the DFEs shown in Figures 1 and 2. Percentage deleterious and beneficial mutations are indicated at the top and bottom of each bar respectively. Panels B–G show different aspects of the mutation spectra of strains. (B) Tv bias (C) Indel bias (D) Noncoding mutation bias (E) Synonymous mutation bias (F) GC→AT bias (note that mutations that do not affect GC→AT bias, i.e., AT→TA and GC→CG mutations, are not shown here) and (G) Types of base-pair substitutions (BPS).

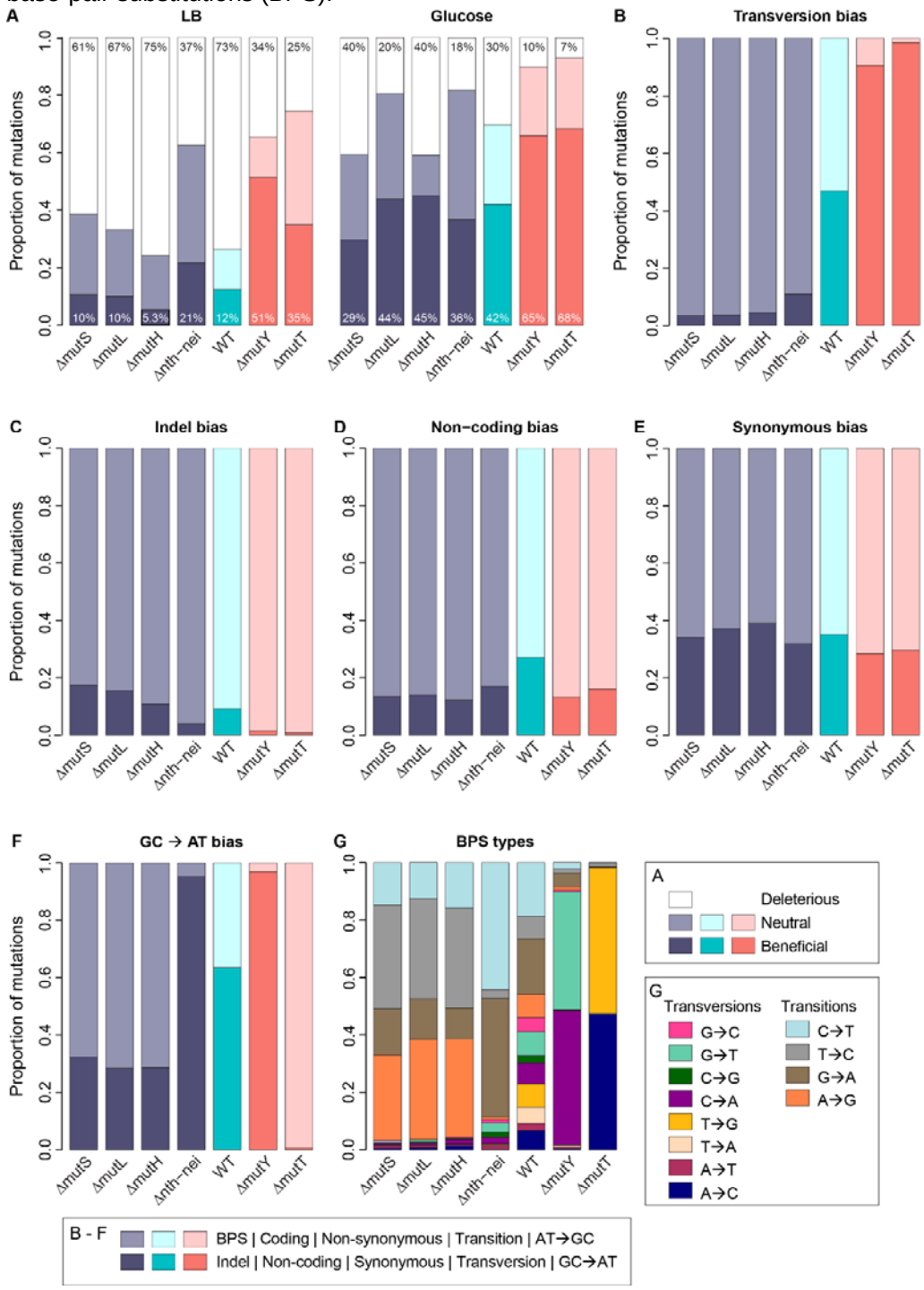

DFE shifts and fraction of beneficial mutations are strongly associated with reversal of Tv bias, with some unexplained variation

The strains used in our analysis differed in several aspects of their mutation spectra (Table 1), so we examined variation in each aspect of the spectrum in more detail (Figures 3B–G). The increase in f_b across strains was positively correlated with the magnitude of Tv bias (i.e., stronger bias reversal) (Figures S3A–B; also compare Figures 3A and 3B). In contrast, no other axis of variation in mutation spectrum matched the pattern of variation in f_b across strains (compare Figure 3A with Figures 3C–F). In each of these cases, either the range of variation in mutation bias across strains was very small (indel bias, synonymous bias, non-coding bias; Figures 3C–E, Table 1) or there was no consistent pattern (noncoding bias and GC→AT bias; Figures 3D and 3F respectively). Even when we considered each type of base substitution separately, the fitness effects and type of mutation were not associated (Figure 3G). For instance, Δ*mutY* and Δ*mutT* each sample distinct types of transversion mutations, yet both have the highest f_b values. Finally, pooling data across all strains in our dataset, transversion mutations were significantly more beneficial than transitions (Figures 4A and 4B), whereas no such fitness difference was observed for any other aspect of the mutation spectrum (except BPS vs. indels in glucose; Figure S5). Together, these results pointed to transversion bias as the dominant cause of DFE differences across strains.

Next, we tested whether the observed associations between transition/transversion bias and fitness effects of mutations are confounded by strain background (i.e., specifically which DNA repair genes were deleted and what other mutations occurred during the genetic manipulations (Supplemental data file S3). We first tested whether higher initial fitness of each strain was associated with lower f_b, reflecting the expected pattern of diminishing returns of beneficial mutations with increasing background fitness [27,28]. Although the fitness of the original deletion strains varied significantly in both media, it was not correlated with f_b (Figure S7). We then conducted pairwise comparisons between strains, considering

only Ts and Tv mutations. We expected that Tv mutations should be generally more beneficial than Ts mutations regardless of strain background, and the same type of mutation (Ts or Tv) should have similar fitness effects in all strain backgrounds. These predictions are broadly borne out in both media (Figures 4A and 4B): Tv mutations in Δ*mutY* and Δ*mutT* had similar (and higher) *s* values than Ts mutations, though in LB the fitness effects of Tv in Δ*mutY* were similar to Ts in WT and in Δ*nth-nei*.

Notably, in some cases Ts mutations in different Ts-biased strains had significantly different fitness effects (Figures 4A and 4B). In LB, Ts mutations in WT and Δ*nth-nei* strains were more beneficial than other Ts-biased strains, and in glucose, Ts in Δ*nth-nei* and Δ*mutL* were more beneficial. These exceptions could potentially be explained by aspects of the mutation spectra other than Ts/Tv bias, but these strains do not stand out as exceptional along other axes of the mutation spectrum (Figures 3B–G, Table 1). Further, comparing Ts-biased strains in each growth medium, we found very few and inconsistent differences in fitness effects along other axes of mutation bias (e.g., coding vs. non-coding, synonymous vs. non-synonymous; Table S6), indicating that they cannot explain the differences in fitness effects across Ts-biased strains. To summarize, the broad patterns of DFE variation that we observed are explained by Ts/Tv bias, but there is additional variation among Ts-biased strains that remains unexplained.

Figure 4: Transversion mutations are more beneficial than transition mutations. Fitness effects of mutations in (A) LB and (B) glucose; sample sizes are shown in x-axis labels in panel A. Note that y-axis ranges differ across panels. In each panel, the first two boxplots compare the effects of all transition vs. transversion mutations, pooled across all strains (asterisks indicate significant differences in Wilcoxon's rank-sum tests; LB: p = 7.7E-10; Glucose: p = 5.1E-10). Following this, boxplots show the fitness effects of only Ts mutations from transition-biased strains and only Tv mutations from transversion-biased strains. Strains with the same letter have similar fitness effects based on paired Wilcoxon's rank sum tests with Benjamini-Hochberg correction (i.e., all strains marked "a" have similar fitness, and all are significantly different from strains marked with "b" or "c". Strains marked "bc" are similar to both "b" and "c"). Comparisons across all other types of mutations are shown in Figure S5.

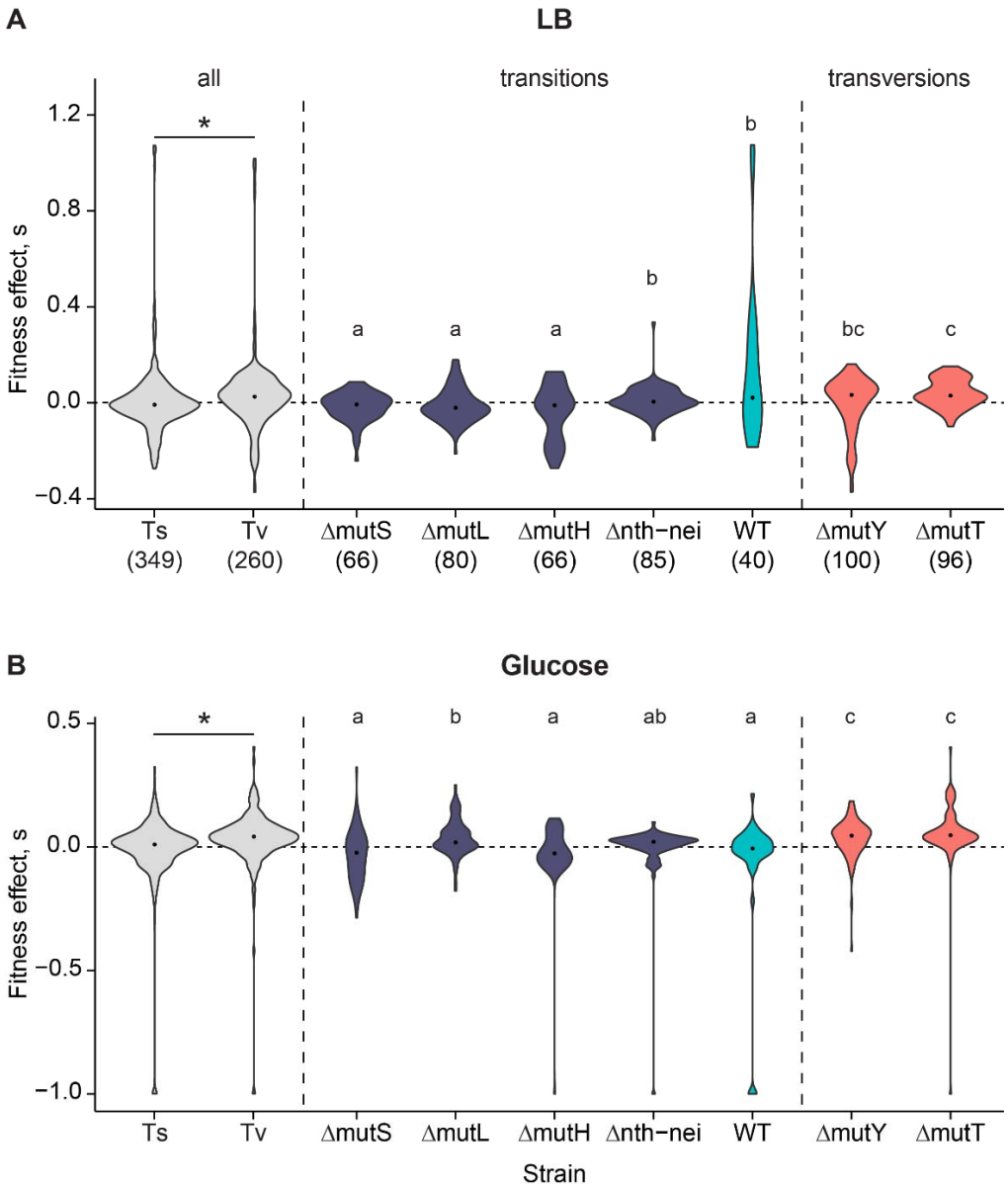

1

Reversal of the GC/AT bias does not alter DFEs

Prior simulations had predicted that the beneficial effects of sampling unexplored mutational space should extend to any axis of the mutation spectrum, including the GC→AT bias [11]. However, here we did not observe the predicted impacts of reversing the GC→AT bias. The WT has a slight GC→AT bias relative to the unbiased expectation of 0.5, and all three MMR strains as well as Δ*mutT* reverse this bias, whereas Δ*mutY* and Δ*nth-nei* strongly reinforce the bias (Table 1, Figure 3F). However, as discussed above, the DFEs of the strains were not correlated with the magnitude of GC→AT bias; and overall, the fitness effects of GC→AT mutations vs. AT→GC mutations were not distinguishable (Figures 5A–B). Since the GC→AT bias varies substantially across genes (Figures S6A–B), we hypothesized that local rather than global bias reversal may be more relevant. However, mutational effects were not correlated with gene GC content regardless of the direction of mutation bias (Figures 5C–D; also see Figures S6C–F). Thus, in contrast to the effects of reversing the Tv bias, neither local nor global GC bias reversal altered the fitness effects of new mutations as predicted by our previous simulations.

Figure 5. Reversal of the GC/AT bias does not impact fitness effects of mutations. Boxplots show fitness effects of AT→GC vs. GC→AT mutations in (A) LB and (B) Glucose. In each plot, data are pooled across all strains; sample sizes (total number of single mutations tested) are shown in the LB panel. 9 mutations that did not alter GC content (i.e., GC→CG or AT→TA mutations) are not shown here. Mutation type did not change fitness effects in either panel (Wilcoxon's rank-sum test; LB: p = 0.4; Glucose: p = 0.24. (C–D) Scatter plots show the relationship between gene GC content and fitness effects of either AT→GC mutations (maroon points) and GC→AT mutations (black points) in (C) LB and (D) Glucose.

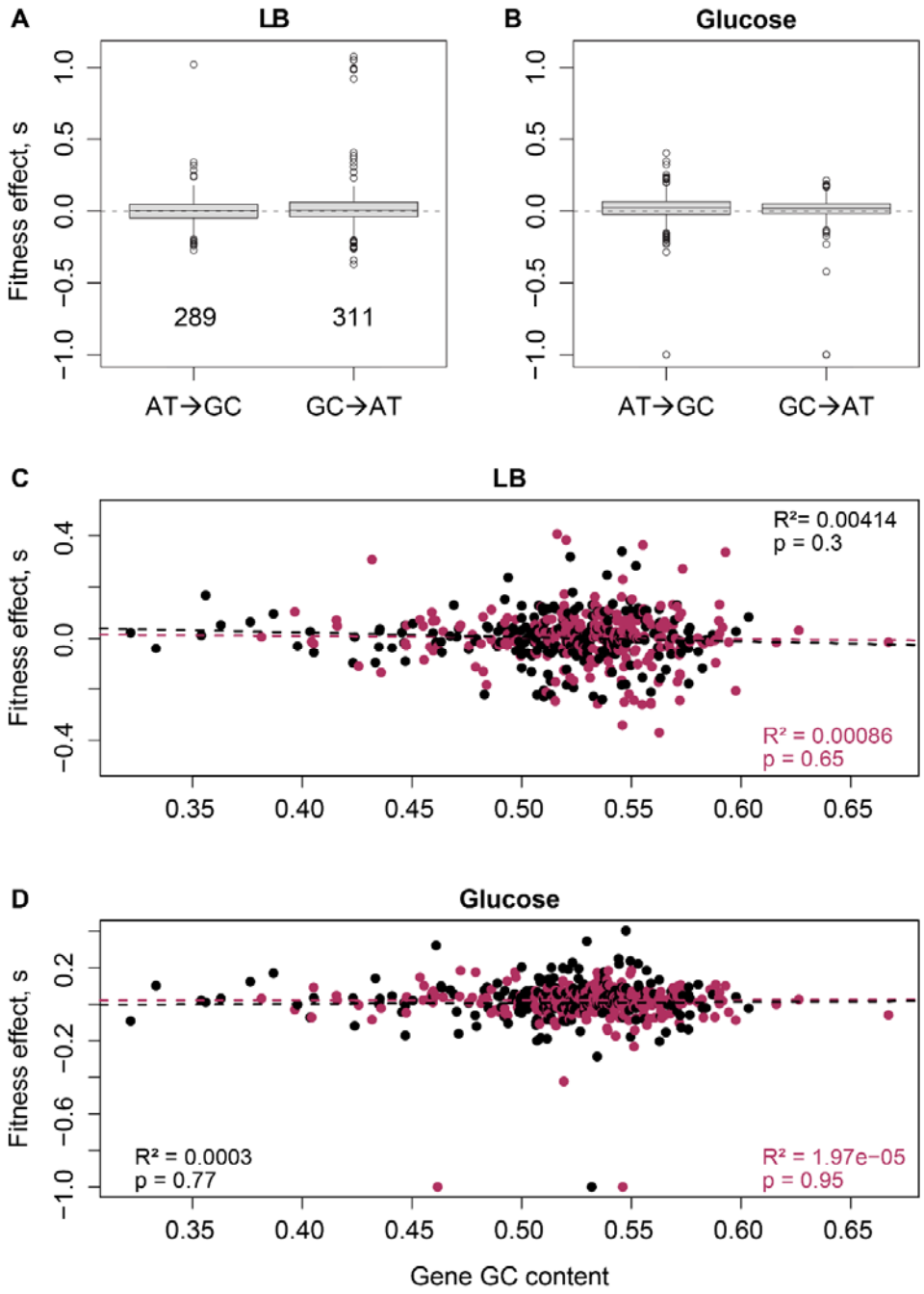

DISCUSSION

Our results represent the first systematic experimental analysis of the fitness consequences of varying mutation bias, and support our prediction that a reversal of an ancestral mutation bias (here, Ts bias in *E. coli*) can lead to a large increase in beneficial mutations. The difference is stark, with Tv-biased strains showing up to ~40% higher f_b relative to Ts-biased strains in both media tested (Figure 3A). Note that even the smallest difference in f_b – 10% for Δ*mutS* vs. 12% for WT in LB – may alter the dynamics of adaptation in large asexual populations, by increasing the overall beneficial mutation rate (e.g., [29]). These results substantially expand upon our prior work, where we observed significantly higher f_b in Δ*mutY* compared to WT in 9 of 16 carbon environments [11]. One unexplained result in the previous study was the lack of significant differences in f_b in five environments, including LB and minimal glucose media. However, in our current analysis with increased sample sizes (80 vs. 94 for WT and 79 vs. 113 for Δ*mutY*), we observed significantly higher f_b in both LB and glucose, suggesting that the previously observed inconsistency across environments may have resulted from low statistical power. Another difference between the two studies is that fitness was measured in slightly different experimental contexts, in 48-well (older study) vs. 96-well microplates (current study). However, this cannot explain the different outcomes for WT and Δ*mutY*, because fitness is strongly positively correlated across microplate types (Figure S8). Finally, in this study we used a narrower definition of neutral mutations (mean experimental measurement error of 0.025, rather than the maximum error value of 0.05 used in the previous study), which could alter the DFE. However, even with the broad definition, WT and Δ*mutY* DFEs were consistently different with the current dataset (Chi-square tests comparing neutral, beneficial, and deleterious proportions; $p<0.01$ in both media). Thus, we suggest that with sufficiently large sample sizes, a Tv bias should consistently lead to right-shifted DFEs in diverse environments for historically Ts-biased species such as *E. coli*.

More generally, our results add to the growing realization that mutation bias can significantly shape evolutionary dynamics [30–32], by providing direct experimental evidence and suggesting a mechanism through which specific types of bias shifts may alter evolutionary outcomes. Earlier work had also suggested that bias shifts can dramatically alter evolutionary dynamics, but the underlying mechanism and interpretations were different [9,10]. These studies showed (using some of the same strains used in our work) that distinct mutation spectra endow strains with differential success in sampling specific antibiotic resistance mutations. As a result, some strains are predicted to adapt faster to specific antibiotics. However, this explanation is specific to particular antibiotics and the relevant mutational targets of resistance. Thus, predicting the relative success of different strains in a given antibiotic would require knowledge of resistance mechanisms and whether they are more likely to arise via a specific type of mutation. In contrast, we provide a more general explanation, predicting that the effect of mutation bias depends on the prior evolutionary history of the population, such that a large shift favoring a previously poorly sampled class of mutations should be generally advantageous [11,12]. We hope that future work will test the effect of specific matches between selection and mutation bias vs. a broad bias reversal, independent of the source of selection. Such analyses are critical to expand our ability to predict adaptive outcomes and mutation fates under diverse selection pressures.

Although our experiments support our prediction about the impact of mutation bias reversals on the DFE, there are some interesting points of divergence. For instance, in LB, Δ*nth-nei* has a larger-than-expected f_b, and the reason is not yet clear. Most intriguing is the variation in the DFEs of three strains with near-identical Ts bias in glucose (Δ*mutH*, Δ*mutL*, Δ*mutS*; Figure 3A), where the same DNA repair pathway (mismatch repair, MMR) is disrupted. Clearly, mutation bias shifts alone cannot explain these differences. One reason could be that some of the deleted DNA repair genes have other functions (apart from DNA repair) that also influence the fitness effects of new mutations. Alternatively, despite attempts to minimize structural disruptions, some repair gene deletions may have caused regulatory

changes in downstream genes, leading to strain-specific epistasis with new mutations. Although we did not observe such epistasis for a set of 19 mutations placed in both WT and Δ*mutY* backgrounds [11], further experiments are necessary to test this hypotheses for genes in the MMR pathway, whose deletion leads to distinct DFEs. Another interesting exception to the effect of Tv bias reversal is that while the overall pattern of change in f_b and f_d is consistent in both media (LB and glucose), we do see media–specific effects. In previous work with WT and Δ*mutY*, we had also observed significant differences in DFEs across environments with different carbon sources [11]. While variation in DFEs across environments is not surprising, the mechanisms underlying change in the rank order of f_b value across environments remain unclear. Analysing the causes of the differences in DFEs across strains with similar mutation bias, as well as across environments, is thus a fruitful avenue for further work.

Another unexplained pattern in our current study is that despite strong reversals and reinforcements of the wild type GC→AT bias in some strains, GC→AT vs. AT→GC mutations had similar fitness effects, and this aspect of the mutation spectrum did not explain variation in the DFE. This is puzzling because simulations had predicted that reversal of *any* aspect of the mutation spectrum should influence the DFE, specifically shown for GC→AT bias [11]. One potential explanation is that the local GC bias rather than genome-wide GC bias is more relevant (e.g., due to the distinct evolutionary history of different genes). A second related hypothesis is that the fitness effects of GC/AT mutations depend strongly on their impact on gene function (e.g., distinct protein-disruptive effects of GC→AT vs. AT→GC mutations), and these effects depend on the genome GC content [33]. However, since we do not see any fitness differences between GC→AT or AT→GC mutations globally or locally (in GC-rich or GC-poor genes), neither hypothesis is supported by our data. A third possibility is that the GC→AT bias varies more frequently and/or dramatically across evolutionary time, reducing the impact of experimentally introduced GC/AT bias reversals relative to Ts/Tv bias reversals. Prior work shows that GC bias is

indeed quite dynamic in the bacterial phylogeny (e.g., [34]), but it is impossible to directly test whether GC bias shifts occur more frequently than Tv bias shifts, because the latter do not leave a genomic signature. However, it is possible to approximately estimate the frequency and direction of bias shifts using the gain and loss of DNA repair genes with known effects on Ts/Tv and GC/AT bias. Using such analysis, we had previously observed that reversals of GC/AT bias occurred more frequently than Ts/Tv in the bacterial phylogeny (see Fig. 5C in [11]). Thus, we speculate that more frequent changes in the genomic GC content may explain why GC bias reversals did not impact the DFE, and emphasize the need for further theoretical and empirical work on the relative effects of bias shifts along different axes of the mutation spectrum.

A striking result from our study is the high proportion of beneficial mutations observed in all strains in glucose, and in transversion-biased strains in LB (Figure 3A), consistent with our previous analysis of WT and Δ*mutY* strains during growth in several carbon sources [11]. As discussed previously by us and by others, such high f_b values are not as rare as generally believed, especially during mutation accumulation studies [11,35]. In a recent review, Bao and colleagues suggest that the widely variable outcomes of fitness decline in MA lines (an indicator of the proportion of deleterious vs. beneficial mutations) is not easily explained by organism, genetic background, or test environment, but may arise from complex interactions between these and/or other factors [35]. In our current study, we ruled out several mechanisms that could artificially inflate the observed f_b values: selection bias during MA (we corrected our DFEs for such bias [15]), low ancestral fitness leading to high f_b values [27,28,36] (we did not find a correlation between ancestral fitness and f_b), and the impact of specific strain backgrounds (we observe a general effect of Ts vs. Tv mutations on f_b). We hope that further analyses will clarify this issue.

Our results also inform several other open questions in the field, such as the fitness consequences of different types of mutational classes. Perhaps most interesting is the lack

of significant differences in the fitness effects of synonymous and nonsynonymous mutations (Figure S5C), adding to the already substantial body of work suggesting that this distinction is not as large or widespread as expected [37,38]. Most prior studies compared the impact of synonymous and non-synonymous changes in specific genes of interest, so our results complement these studies in showing similar fitness effects across hundreds of mutations across the genome. Similarly, we do not find significant differences in coding vs. noncoding mutations (Figure S5B), or AT→GC vs. GC→AT mutations (Figure S5D). Together, our results indicate that while the fitness consequences of each of these types of mutations is probably highly context-specific, such patterns are not observed at the genome-wide scale (i.e., the fitness effect of mutations varies across sites or genomic locations). Future studies with larger sample sizes conducted in different environmental contexts and with distinct organisms will be valuable to test the generality of our results.

The demonstration of large shifts in the distribution of mutational effects as a result of altered mutation bias has important implications for evolutionary dynamics. One prediction is that changes in mutation spectra across environments or populations – observed in diverse taxa [39–44] – could lead to distinct DFEs in each case, influencing evolutionary dynamics. A second important implication is regarding the evolution of mutators, which have dysfunctional DNA repair and high mutation rates that can facilitate rapid sampling of beneficial mutations [45]. Most mutators also have distinct mutation biases (e.g., except the WT, all strains used in this study are mutators), but the evolutionary implications of such bias shifts in mutators have been only rarely considered [33]. We suggest that the large DFE shifts that we observe – with concomitant changes in the beneficial mutation supply and deleterious load of mutators – can alter the rate and nature of adaptation in new environments. Accounting for these DFE shifts is thus critical to allow more accurate predictions of the fates of mutators with altered mutation biases in populations under selection. Indeed, a recent analytical and simulation study predicts that right-shifted DFEs driven by mutation bias shifts can significantly enhance the ability of mutator strains to

invade non-mutator populations [12]. Thus, some mutators could gain an additional advantage – over and above the effect of high mutation rate – if their mutation bias opposes that of the ancestor. Mutators are observed frequently in natural microbial populations as well as in clinical settings, where they are often associated with drug resistance [46,47]. Testing the impacts of mutation bias shifts on evolutionary dynamics is thus a promising direction for future research.

ACKNOWLEDGEMENTS

We thank Pratibha Sanjenbam and Lindi Wahl for critical comments on the manuscript; Lindi Wahl for discussion; Kushan Lahiri for laboratory assistance; and the NGS facility for sequencing. We acknowledge funding and support from the National Centre for Biological Sciences (NCBS–TIFR) and the Department of Atomic Energy, Government of India (Project Identification No. RTI 4006), and the University Grants Commission, India (fellowship number 211610044747 to SP).

AUTHOR CONTRIBUTIONS

MS and DA conceived of the project and designed the work; DA acquired funding; MS and SP conducted experiments and analysed data; MS and DA interpreted the results; DA wrote the manuscript with input from all authors.

REFERENCES

1. Eyre-Walker A, Keightley PD. The distribution of fitness effects of new mutations. Nature Reviews Genetics. 2007;8: 610–618. doi:10.1038/nrg2146
2. Bataillon T, Bailey SF. Effects of new mutations on fitness: insights from models and data. Fox CW, Mousseau TA, editors. Annals of the New York Academy of Sciences. 2014;1320: 76–92. doi:10.1111/nyas.12460
3. Chen J, Bataillon T, Glémin S, Lascoux M. What does the distribution of fitness effects of new mutations reflect? Insights from plants. New Phytol. 2022;233: 1613–1619. doi:10.1111/nph.17826
4. Wortel MT, Agashe D, Bailey SF, Bank C, Bisschop K, Blankers T, et al. Towards evolutionary predictions: Current promises and challenges. Evol Appl. 2023;16: 3–21. doi:10.1111/eva.13513
5. Agashe D, Sane M, Singhal S. Revisiting the Role of Genetic Variation in Adaptation. Am Nat. 2023; 000–000. doi:10.1086/726012
6. Charmouh AP, Bocedi G, Hartfield M. Inferring the distributions of fitness effects and proportions of strongly deleterious mutations. G3: Genes, Genomes, Genet. 2023. doi:10.1093/g3journal/jkad140
7. Stearns FW, Fenster CB. The effect of induced mutations on quantitative traits in Arabidopsis thaliana: Natural versus artificial conditions. Ecol Evol. 2016;6: 8366–8374. doi:10.1002/ece3.2558
8. Katju V, Bergthorsson U. Old trade, new tricks: Insights into the spontaneous mutation process from the partnering of classical mutation accumulation experiments with high-throughput genomic approaches. Makova K, editor. Genome Biology and Evolution. 2018;11: 136–165. doi:10.1093/gbe/evy252
9. Couce A, Guelfo JR, Blázquez J. Mutational spectrum drives the rise of mutator bacteria. PLoS Genetics. 2013;9: e1003167. doi:10.1371/journal.pgen.1003167
10. Couce A, Rodríguez-Rojas A, Blázquez J. Bypass of genetic constraints during mutator evolution to antibiotic resistance. Proceedings Biological sciences / The Royal Society. 2015;282: 20142698–9. doi:10.1098/rspb.2014.2698
11. Sane M, Diwan GD, Bhat BA, Wahl LM, Agashe D. Shifts in mutation spectra enhance access to beneficial mutations. Proc National Acad Sci. 2023;120: e2207355120. doi:10.1073/pnas.2207355120
12. Tuffaha MZ, Varakunan S, Castellano D, Gutenkunst RN, Wahl LM. Shifts in mutation bias promote mutators by altering the distribution of fitness effects. Am Nat. 2023. doi:10.1086/726010

13. Foster PL, Lee H, Popodi E, Townes JP, Tang H. Determinants of spontaneous mutation in the bacterium Escherichia coli as revealed by whole-genome sequencing. Proceedings of the National Academy of Sciences of the United States of America. 2015; 201512136–10. doi:10.1073/pnas.1512136112
14. Sane M, Miranda JJ, Agashe D. Antagonistic pleiotropy for carbon use is rare in new mutations. Evolution. 2018;72: 2202–2213. doi:10.1111/evo.13569
15. Wahl LM, Agashe D. Selection bias in mutation accumulation. Evolution. 2022;76: 528–540. doi:10.1111/evo.14430
16. Mahilkar A, Raj N, Kemkar S, Saini S. Selection in a growing colony biases results of mutation accumulation experiments. Sci Rep-uk. 2022;12: 15470. doi:10.1038/s41598-022-19928-5
17. Baba T, Ara T, Hasegawa M, Takai Y, Okumura Y, Baba M, et al. Construction of Escherichia coli K-12 in-frame, single-gene knockout mutants: the Keio collection. Molecular Systems Biology. 2006;2: 2460–11. doi:10.1038/msb4100050
18. Thomason LC, Costantino N, Court DL. E. coli genome manipulation by P1 transduction. John Wiley & Sons, Inc.; 2001. doi:10.1002/0471142727.mb0117s79
19. Deatherage DE, Barrick JE. Identification of mutations in laboratory-evolved microbes from next-generation sequencing data using breseq. Methods in molecular biology (Clifton, NJ). 2014;1151: 165–188. doi:10.1007/978-1-4939-0554-6_12
20. Li H, Handsaker B, Wysoker A, Fennell T, Ruan J, Homer N, et al. The Sequence Alignment/Map format and SAMtools. Bioinformatics. 2009;25: 2078–2079. doi:10.1093/bioinformatics/btp352
21. Koboldt DC, Chen K, Wylie T, Larson DE, McLellan MD, Mardis ER, et al. VarScan: variant detection in massively parallel sequencing of individual and pooled samples. Bioinformatics. 2009;25: 2283–2285. doi:10.1093/bioinformatics/btp373
22. Delaney NF, Kaczmarek ME, Ward LM, Swanson PK, Lee M-C, Marx CJ. Development of an optimized medium, strain and high-throughput culturing methods for Methylobacterium extorquens. Zhang Q, editor. PLoS ONE. 2013;8: e62957. doi:10.1371/journal.pone.0062957
23. Raynes Y, Sniegowski PD. Experimental evolution and the dynamics of genomic mutation rate modifiers. Heredity. 2014;113: 375–380. doi:10.1038/hdy.2014.49
24. Sniegowski PD, Gerrish PJ, Lenski RE. Evolution of high mutation rates in experimental populations of E. coli. Nature. 1997;387: 703–705. doi:10.1038/42701
25. Taddei F, Radman M, Maynard-Smith J, Toupance B, Gouyon PH, Godelle B. Role of mutator alleles in adaptive evolution. Nature. 1997;387: 700–702. doi:10.1038/42696
26. Wielgoss S, Barrick JE, Tenaillon O, Wiser MJ, Dittmar WJ, Cruveiller S, et al. Mutation rate dynamics in a bacterial population reflect tension between adaptation and genetic

load. Proceedings of the National Academy of Sciences. 2013;110: 222–227. doi:10.1073/pnas.1219574110

27. Khan AI, Dinh DM, Schneider D, Lenski RE, Cooper TF. Negative epistasis between beneficial mutations in an evolving bacterial population. Science. 2011;332: 1193–1196. doi:10.1126/science.1203801

28. Chou HH, Chiu HC, Delaney NF, Segre D, Marx CJ. Diminishing returns epistasis among beneficial mutations decelerates adaptation. Science. 2011;332: 1190–1192. doi:10.1126/science.1203799

29. Good BH, Rouzine IM, Balick DJ, Hallatschek O, Desai MM. Distribution of fixed beneficial mutations and the rate of adaptation in asexual populations. Proceedings of the National Academy of Sciences. 2012;109: 4950–4955. doi:10.1073/pnas.1119910109

30. Stoltzfus A. Mutation, Randomness and Evolution. Oxford University Press; 2021.

31. Stoltzfus A, Yampolsky LY. Climbing Mount probable: Mutation as a cause of nonrandomness in evolution. Journal of Heredity. 2009;100: 637–647. doi:10.1093/jhered/esp048

32. Horton JS, Taylor TB. Mutation bias and adaptation in bacteria. Microbiology. 2023;169. doi:10.1099/mic.0.001404

33. Couce A, Tenaillon O. Mutation bias and GC content shape antimutator invasions. Nature communications. 2019;10: 3114–9. doi:10.1038/s41467-019-11217-6

34. Mahajan S, Agashe D. Evolutionary jumps in bacterial GC content. G3 Genes Genomes Genetics. 2022; jkac108. doi:10.1093/g3journal/jkac108

35. Bao K, Melde RH, Sharp NP. Are mutations usually deleterious? A perspective on the fitness effects of mutation accumulation. Evol Ecol. 2022; 1–14. doi:10.1007/s10682-022-10187-4

36. Kryazhimskiy S, Rice DP, Jerison ER, Desai MM. Microbial evolution. Global epistasis makes adaptation predictable despite sequence-level stochasticity. Science. 2014;344: 1519–1522. doi:10.1126/science.1250939

37. Agashe D. Evolutionary Forces That Generate SNPs: The Evolutionary Impacts of Synonymous Mutations. In: Sauna ZE, Kimchi-Sarfaty C, editors. Single Nucleotide Polymorphisms: Human variation and a coming revolution in biology and medicine. Cham, Switzerland: Springer; 2022. pp. 15–36. doi:10.1007/978-3-031-05616-1

38. Bailey SF, Morales LAA, Kassen R. Effects of synonymous mutations beyond codon bias: The evidence for adaptive synonymous substitutions from microbial evolution experiments. Genome Biol Evol. 2021. doi:10.1093/gbe/evab141

39. Liu H, Zhang J. Yeast Spontaneous Mutation Rate and Spectrum Vary with Environment. Curr Biol. 2019;29: 1584-1591.e3. doi:10.1016/j.cub.2019.03.054

40. Shewaramani S, Finn TJ, Leahy SC, Kassen R, Rainey PB, Moon CD. Anaerobically grown Escherichia coli has an enhanced mutation rate and distinct mutational spectra. Cooper VS, editor. PLoS Genetics. 2017;13: e1006570-22. doi:10.1371/journal.pgen.1006570

41. Harris K, Pritchard JK. Rapid evolution of the human mutation spectrum. eLife. 2017;6: e24284. doi:10.7554/elife.24284.001

42. Maharjan RP, Ferenci T. A shifting mutational landscape in 6 nutritional states: Stress-induced mutagenesis as a series of distinct stress input–mutation output relationships. Gore J, editor. PLoS Biology. 2017;15: e2001477-22. doi:10.1371/journal.pbio.2001477

43. Maharjan RP, Ferenci T. The impact of growth rate and environmental factors on mutation rates and spectra in Escherichia coli. Environmental Microbiology Reports. 2018;10: 626–633. doi:10.1111/1758-2229.12661

44. Hasan AR, Lachapelle J, El-Shawa SA, Potjewyd R, Ford SA, Ness RW. Salt stress alters the spectrum of de novo mutation available to selection during experimental adaptation of Chlamydomonas reinhardtii. Evolution. 2022;76: 2450–2463. doi:10.1111/evo.14604

45. Sniegowski PD, Gerrish PJ, Johnson T, Shaver A. The evolution of mutation rates: separating causes from consequences. BioEssays. 2000;22: 1057–1066. doi:10.1002/1521-1878(200012)22:12<1057::aid-bies3>3.0.co;2-w

46. Oliver A, Cantón R, Campo P, Baquero F, Blázquez J. High Frequency of Hypermutable Pseudomonas aeruginosa in Cystic Fibrosis Lung Infection. Science. 2000;288: 1251–1253. doi:10.1126/science.288.5469.1251

47. Gifford DR, Berríos-Caro E, Joerres C, Suñé M, Forsyth JH, Bhattacharyya A, et al. Mutators can drive the evolution of multi-resistance to antibiotics. PLOS Genet. 2023;19: e1010791. doi:10.1371/journal.pgen.1010791

48. Friedberg EC, Elledge SJ, Lehmann AR, Lindahl T, Muzi-Falconi M, editors. DNA Repair, Mutagenesis, and Other Responses to DNA Damage: A Subject Collection from Cold Spring Harbor Perspectives in Biology. USA: Cold Spring Harbor Laboratory Press; 2013.